An Evaluation of Back Stress Determination Techniques in Metals

W.B. Jones, R.W. Rohde
Sandia National Laboratories, Org. 1835, P.O. Box 5800, Albuquerque, New Mexico 87185, U.S.A.

SUMMARY

The desire to develop unified creep-plasticity (UCP) models comes from the necessity to design advanced nuclear reactor components for service under conditions which include combined creep and low cycle fatigue. These models should also be physically based since they would be used to extrapolate from laboratory data to predict long service lives. An approach to UCP modeling centers on the hypothesis that the inelastic strain rate is determined by a balance between the competing processes of work hardening and recovery. One class of UCP models is characterized by a power law relationship between strain rate and stress. A state variable common to these models characterizes the isotropic hardening and is allowed to evolve with history according to simultaneous work hardening and recovery. In order to treat behaviors unique to unloading or reverse loading conditions, several models also include a kinematic hardening variable which is also allowed to evolve according to a balance of work hardening and recovery. Such a treatment of inelastic deformation can mathematically treat a wide variety of behaviors. The measured response of 316SS and A800 indicates that the kinematic variable must, in steady state, be taken as a constant fraction (about 0.8) of the applied stress. This experimental result makes it impossible for the simple power law type expression to properly predict the commonly observed power law breakdown behavior in most metals and alloys. It is proposed that an expression for total inelastic strain rate involving the sum of two separate strain rate contributions is more appropriate. Acknowledging that separate expressions and separate mechanisms dominate low stress (engineering service) conditions and high stress (laboratory test) conditions requires that more emphasis be placed on long time, low stress laboratory testing.

---

*This work performed at Sandia National Laboratories by the U.S. Department of Energy under contract number DE-AC04-76DP00789.
**A U.S. DOE facility.

1. Introduction

The desire to develop unified creep-plasticity (UCP) models comes from the necessity to design advanced nuclear reactor components for service under conditions which include creep and low cycle fatigue. To develop such models involves the challenge of not only properly treating time independent and time dependent deformation, but also properly treating reversed cyclic loading histories. Superposed on these requirements is the fact that relatively short time mechanical property data must be used to design components for 30 year life. This demands that the models reflect a reasonable physical basis appropriate to the mechanisms of deformation for each alloy.

An approach to UCP modeling centers on the hypothesis that the inelastic strain rate is determined by a balance between the competing processes of work hardening and recovery. One class of UCP models is characterized by a power law relationship between strain rate and stress and has been reviewed by Krieg [1]. One state variable present in these models characterizes the isotropic hardening and is made to evolve with history according to simultaneous work hardening and recovery. Several models also treat kinematic hardening using a second state variable which will be termed the kinematic variable. This second variable is also allowed to evolve with history according to a work hardening/recovery balance.

Power law models then have a general form:

$$\dot{\varepsilon} = C_1 \left| \frac{F(\sigma-\alpha)}{R} \right|^n \qquad (1)$$

where $\dot{\varepsilon}$ is the inelastic strain rate, σ is the applied stress, α is the kinematic variable, and R is the isotropic hardening variable. In many models, the stress function is simply its argument, or:

$$\dot{\varepsilon} = C_1 \left| \frac{(\sigma-\alpha)}{R} \right|^n \qquad (2)$$

The isotropic hardening variable here is usually proportional to the current yield stress and is measured in loading/unloading tests. The kinematic variable represents the movement of the yield surface away from the origin in stress space and is most often measured using the strain transient dip test [2] although full stress reversal tests have also been used [3]. The kinematic variable is necessary to model the cyclic behavior of alloys. The stress exponent n is a material constant and not stress dependent. For this form of deformation model to have a physical basis, the value of that exponent must be less than about 5 [4]. We will show in this paper that measured values of the kinematic variable make it impossible to use an equation of the form of eq. (2). These results indicate that the change in deformation mechanism indicated by such phenomena as "power law breakdown" must be treated in the stress function of eq. (1) and not in the evolutionary form for either the kinematic or isotropic hardening variables. Solid solution hardening effects are shown to dominate the nature of the observed strain transients and must therefore be incorporated in the evolutionary form of the isotropic hardening variable.

2. Materials

Two commercial alloys have been examined in this study: AISI 316 stainless steel and Alloy 800. Both of these alloys are commonly used in elevated temperature applications and both have been proposed as candidate alloys for advanced nuclear reactor and solar central receiver applications. Table I summarizes the heat treatment of the alloys used.The difference in grain size in the two heats of A800 results in significant differences in the mechanical behavior of the alloy. The larger grain size in both the 316SS and heat 8144 of A800 results in improved creep resistance [5] while the fatigue resistance is not much influenced. In both of these alloys, long time at temperatures in excess of 800 K results in microstructural changes involving carbide and other precipitate formation [6,7]. The tests conducted here did not extend into the time regime at which these changes become significant. However, in terms of deformation modeling used to predict the behavior a structure in elevated temperature service, such microstructural evolution would have to be incorporated in the predictions.

The specimens tested here had a cylindrical gage section 6.35 mm in diameter and 52 mm in length. All were tested in the annealed condition.

3. Strain Transient Dip Test Technique

A specially designed dead weight machine was used to determine the strain transient response of these alloys after incremental unloading. This apparatus has been described in detail elsewhere [8]. The load is decremented by lifting either one of the two dip trays off the load train using pneumatically driven jacks. In order that the load train be as rigid as possible, direct loading was used which precluded the use of a constant stress cam. Instead, to approximate constant stress conditions, the weight on the main load tray was adjusted regularly according to changes in cross sectional area. Since the creep rates encountered were all less than $1 \times 10^{-3} s^{-1}$, each correction was small.

A three zone split tube furnace was used for heating. It is capable of maintaining a temperature constant to within ± 0.1 K over the several hours of transient behavior after a load change, and constant within ± 0.2 K of the test temperature over the entire period of the creep test. This temperature variation would appear as ± 2 $\mu\varepsilon$. The strain transient response was measured using a modified axial rod linear variable differential transformer (LVDT) extensometer. This extensometer system produces a strain resolution of about 5 $\mu\varepsilon$. The strain and load data were recorded in two ways. A Nicolet digital storage oscilloscope was used to follow the short time transient response (20 s) and a Honeywell thermal pen strip chart recorder was used as a continuous monitor of the strain in each test. The step unloading occurs at a rate of about 1 MPa/ms with 10 to 20 pct load overshoot followed by decaying oscillations. These are natural frequency oscillations of the specimen having a period of about 40 ms and a decay time of about 2 s.

4. Data Reduction

The specimens were heated to the chosen test temperature and a load applied (σapl). The step unloadings were conducted after the minimum creep rate was attained. Numerous step unloadings were preformed between 10 and 70 MPa for each applied load and the strain transient response recorded. The kinematic variable has been determined from these data using a new technique proposed by Blum and Finkel [9], rather than the originally proposed technique of examining the data for periods of zero creep rate after unloading [2]. The inherent difficulties in determining zero creep rates have been shown by Jones, et al [8], difficulties which are alleviated by use of the Blum and Finkel technique. Figure 1 shows a typical strain-time transient curve for the alloys studied here. The instantaneous strain change is defined by $\varepsilon_0 - \varepsilon_1$ and the maximum strain change by $\varepsilon_0 - \varepsilon_2$. For small unloading steps, the value of these two will be equal while for large unloading steps the time dependent negative backflow component will cause the two values to be different. When these strain changes are plotted against the corresponding stress decrements, curves similar to Figure 2 are produced. The point at which the two curves converge (σ^*) defines the kinematic variable for that applied stress according to $\alpha = \sigma\text{apl} - \sigma^*$.

5. Results

The creep behaviors characteristic of 316SS and A800 are shown in Figure 3. In all cases, instantaneous straining was followed by a decreasing strain rate primary creep regime. True steady state creep was not observed; however, near minimum creep rates were observed over several hundred hours in many cases. The minimum creep rate data were analyzed using an expression of the form:

$$\dot{\varepsilon} = A \exp(-Q/RT) \left[\frac{\sigma_{apl}}{E}\right]^{n} \qquad (3)$$

where σapl is the applied stress, R is the gas constant, T is the temperature, n' is the stress exponent, and Q is an apparent activation energy. At both 922 and 977 K, the large grained A800 (heat 8144) had n'= 17 and Q = 410 kJ/mole. The small grained A800 (heat 8523) had n'= 6 and Q = 270 kJ/mole.

The 316SS had n'= 20 and Q = 380 kJ/mole. These tests were conducted at homologous temperatures ranging from 0.50 to 0.54 and a modulus normalized stress range from 0.5 $x10^{-3}$ to 1.5 x 10^{-3}. Morris [10] has conducted creep tests on 316SS at 898 K and found the effective stress exponent increased from about 7 to 16 across the stress range investigated in the present work. Similarly, Tavassoli [11] found stress exponents ranging from about 4 to 20 for A800 tested in the temperature range 773-823 K. This rapid increase in stress exponent at about a modulus compensated stress level of 10^{-3} is typical of most metals and alloys and has been termed power law breakdown [5].

Figure 1 shows the major features characteristic of the strain transients after step unloading in both A800 and 316SS. Region A is the instantaneous contraction that occurs during the unloading. The effective modulus, $\Delta\sigma/\Delta\varepsilon$, calculated from these unloadings was consistently less than the Young's modulus determined from dynamic measurements [12]. Blum and Finkel [9] have observed similar behavior in aluminum and aluminum alloys. When these unloading strain decrements were compared with the instantaneous reloading strain increments which followed each dip, no differences were found. Solid solution alloys of aluminum have been found to exhibit this behavior [13,14] while pure aluminum produces larger strain increments on reloading than decrements with unloading [13]. This different behavior has been interpreted as reflecting the viscous motion of dislocations in solid solution alloys compared to free flight motion of dislocations in pure metals [14].

The region labeled B in Figure 1 is the critical portion of the total transient in determining the kinematic variable. All the step unloadings in this study were continued long enough to clearly determine the maximum strain change. Using the values of instantaneous and maximum strain change according to the procedure described earlier, the kinematic variable has been calculated and the results shown in Figure 4. They have been plotted as the ratio α/σ versus σ/E. Limited work has been performed on similar alloys and those results are also shown in Figure 4. The results of Ziaai-Moayyed [15] for 304SS are lower than those developed here but each set indicates that the ratio α/σ is essentially stress independent. The tests on 304SS were torsion tests and the data were reduced using the zero strain rate criterion. The results of Milicka [16] for solution annealed A800 are in reasonable agreement and also indicate that the ratio α/σ is constant over this range of applied stresses.

After the maximum strain decrement had been reached, the strain increased through a transient toward the creep rate appropriate to the current stress. This period, marked C in Figure 1, was a decreasing strain rate transient for both alloys studied. The transients observed after reloading, however, showed an increasing strain rate. This is typical of the behavior of solid solution strengthened alloys [17]. This observation together with the measured equality of the instantaneous unloading and reloading strains indicates that solid solution strengthening effects must be included in any interpretation of these transients. This form of transient creep behavior was a bit surprising considering that Figure 3 shows that, during the initial loading, the primary creep transient was not characteristic of solid solution strengthening. This indicates that the mechanism controlling deformation of the annealed material with a very low dislocation density is not the same mechanism controlling the response of the alloy after a stable substructure has been established.

Earlier work [12] has established that both of these alloys display fading memory of their mechanical histories. Accordingly, the strain rates which evolve in region D of Figure 1 are the same as the strain rates which would develop in an annealed specimen tested at the decremented load value.

6. Discussion

The strengths of the unified creep-plasticity can be twofold: first, the presence of both an isotropic and a kinematic variable allows cyclic deformation to be modeled, and second, the use of work hardening and recovery terms in the evolution of these variables allows time dependent transients to be modeled. However, our results showed that the specific power law form for a UCP model given in eq. (2) is incorrect. Let us examine how this form of deformation model treats steady state creep behavior.

Experimental results for pure metals and alloys [5] tested at about half of the melting temperature indicates that the effective stress exponent $n' = d(\ln\dot{\varepsilon})/d(\ln\sigma)$ increases with increasing stress. In many materials, a relatively constant value of 4 to 6 is maintained below stresses of about $\sigma/E = 10^{-3}$. Above this stress level, the exponent increases to values as large as 20 to 30 and has been called the power law breakdown region. Unfortunately, the most reasonable laboratory test conditions fall in this region while the service conditions are typically at much lower stresses. This requires that the deformation models used for design be able to appropriately span this range of conditions to produce reasonable long-time deformation and failure predictions.

The parameter n in eq. (1) and eq. (2) must be a material constant and not a function of stress. This demands that the effective exponent, n', be stress dependent through the functional forms of the two state variables R and α. For steady state behavior, these variables are considered to be at steady state values. The isotropic hardening variable can be stress dependent through several mechanisms. In pure materials when only dislocation substructure strengthening is present, hardening occurs in relation to such microstructural features as dislocation density cell size and mean free dislocation path. However, it has been shown [4] that such hardening would have an insufficient effect on the stress dependence of the isotropic hardening variable to account for power law breakdown. Alternately in solid solution alloys there is some evidence that the additional hardening obtained by solute-dislocation interaction may give the hope of constructing an isotropic variable which could explain power law breakdown in these alloys [18]. Consistency, however, demands that the variable used to treat power law breakdown be the same in both pure metals and alloys. In this case the isotropic variable fails as such a modeling tool.

The kinematic variable, by contrast, has been used to account for power law breakdown in several materials [19,20]. In each of these cases, the kinematic variable was visualized as a microstructurally based back stress or internal stress which diminished the effective stress acting on the dislocations in the alloy. The form of eq. (2) dictates that the ratio (α/σ) must decrease with increasing stress to simulate the power law breakdown behavior. Early strain transient dip tests on pure Al and Al-Mg alloys [19] seemed to give this result and the stress exponent could be adjusted downward to the mechanistically satisfying value of 3. A similar approach has been proposed for several engineering alloys [20] where experiments seemed to indicate that the back stress ratio decreased with increasing applied stress. However, the work of Blum and Finkel [9] and Jones and Rohde [8] indicates that when properly analyzed, the dip test data show that the ratio (α/σ) is very nearly independent of applied stress. In this event, the kinematic variable has no effect on the apparent stress exponent and cannot account for power law breakdown.

The dilemma posed by these experimental results is that there appears to be no straightforward way to treat the power law breakdown behavior common to most materials using a deformation model like eq. (2). From the analytical perspective, the approach taken by Miller [3] is attractive. The MATMOD model uses a sinh function according to:

$$\dot{\varepsilon} = C_1 \left| \frac{\mathrm{Sinh}(\sigma-\alpha)}{R} \right|^5 \qquad (4)$$

This equation produces a constant stress exponent of 5 at lower stresses and an exponential behavior at higher stresses to represent power law breakdown; however it is a phenomenological expression which lacks a clear physical justification.

Nix and Ilschner [17] have proposed that the heterogeneous nature of the dislocation substructure which develops with deformation allows the inelastic strain rate to be written as:

$$\dot{\varepsilon} = \dot{\varepsilon}_h + \dot{\varepsilon}_s \qquad (5)$$

where e_h is the strain rate occurring in the hard (cell wall) regions and e_s is the strain rate occurring in the soft (cell center) regions. The heterogeneity of the microstructure allows these two contributions to be summed and the larger of the two to dominate the observed response. If creep in one of the regions is characterized by diffusion controlled recovery, then that contribution will be a power law type expression [17]. If the deformation in the other region is controlled by thermally activated glide, then that strain rate expression will be an exponential expression. Typically, at low temperature and high stresses, thermally activated glide is easier and the total strain rate would show exponential behavior. Conversely, at higher temperatures and lower stresses diffusion controlled recovery dominates and a power law relation with a stress exponent of about 4 would be present. This approach has been used by Blum to rationalize the creep of pure Al in the power law breakdown region [21]. Assuming that the deformation was dominated by thermally activated glide, he approximated the total strain rate by:

$$\dot{\varepsilon} = C_2 \exp(\sigma \Delta a b / MkT) \qquad (6)$$

where b is the Burgers vector, Δa is the activation area, M is the Taylor factor and kT have their usual meanings. Using reasonable values for these parameters, good agreement was found with the creep test data. When fit to a power law, the stress exponent for those data was $n' = 12$.

To be applicable to either 316SS or A800, a deformation model based on eq. (5) would have to incorporate solid solution strengthening effects. In general, it would be possible to have viscous drag by solutes limiting the strain rate in either or both the hard and soft regions of the microstructure. Isotropic hardening terms, possibly similar to those proposed by Schmidt and Miller [18], should be present in both terms of eq. (5).

The application of the approach summarized in eq. (5) would put severe constraints on the test conditions used to characterized alloy behavior. Because separate deformation mechanisms are treated in separate terms of the the UCP model, test conditions which produce the dominance of each mechanism must be chosen. This would be necessary to insure that conditions involving a balanced contribution from both mechanisms have been treated properly. For mechanical property testing, this indicates that a few tests at low stresses may be more valuable than a large number of tests at higher stresses.

7. Conclusions

Measurements of the kinematic variable in A800 and 316SS indicate that the ratio (α/σ) is approximately stress independent and has a value over 0.8 at $\sigma/E = 1 \times 10^{-3}$ in the temperature range 922 to 977 K.

UCP models using a simple power law expression to predict strain rate response cannot treat the power law breakdown behavior characteristic to metals and alloys. An expression involving the sum of two strain rate contributions is suggested to alleviate the limitations of the power law expression along.

Acknowledging that low stress (engineering service) conditions are dominated by a different deformation mechanism that higher stress (laboratory test) conditions requires that more consideration be given to conducting the long lived, low stress creep tests in the laboratory. This may be the only method to knowledgeably characterize the low stress response of metals and alloys.

8. References

1. KRIEG, R.D., Proceedings Fourth Intl. Conf. on Structural Mechanics in Reactor Technology, San Fransisco, 1977, Paper M 6/4.

2. AHLQUIST, C.N., NIX, W.D., Scripta Met. 3, 679-681 (1969).

3. MILLER, A., J. of Eng. Matls. and Tech. 98, 97 (1976).

4. KOCKS, U.F., ARGON, A.S., ASHBY, M.F., Thermodynamics and Kinetics of Slip, Pergamon Press, New York (1975).

5. MUKHERJEE, A.K., "High Temperature Creep", Treatise on Materials Science and Technology Volume 6, Academic Press, New York (1975).

6. WEISS, B., STICKLER, R., Met. Trans. 3, 851 (1972).

7. JONES, W.B., ALLEN, R.E., Met. Trans. A 13A, 637 (1982).

8. JONES, W.B., ROHDE, R.W., SWEARENGEN, J.C., "Deformation modeling and the Strain Transient Dip Test", Mechanical Testing for Deformation Model Development, ASTM STP 765, ASTM, Philadelphia (1982).

9. BLUM, W., FINKEL, A., Acta Metall. 30, 1705 (1982).

10. MORRIS, D.G., Acta Metall. 26, 1143 (1978).

11. TAVASSOLI, A.A., Nuclear Engr. and Design 54, 279 (1979).

12. JONES, W.B., ROHDE, R.W., "Measuring Back Stresses in Commercial Alloys at Elevated Temperatures" Novel Techniques in Metal Deformation Testing, AIME, Warren, Ohio (1983).

13. OIKAWA, H., SUGAWARA, K., Scripta Metall. 12, 85 (1978).

14. OIKAWA, H., Phil. Mag. A 37, 707 (1978).

15. ZIAAI-MOAYYED, A.-A., "Back Stresses in Monotonic and Cyclic Deformation: Transient and Steady State Behavior", Ph.D. Dissertation Stanford University (1981).

16. MILICKA, K., Metal Science 16, 419 (1982).

17. NIX, W.D., ILSCHNER, B., "Mechanisms Controlling Creep of Single Phase Metals and Alloys", Strength of Metals and Alloys, Pergamon Press, New York (1980).

18. SCHMIDT, C.G., MILLER, A.K., Acta Metall. 30, 615 (1982).

19. EVANS, W.J., HARRISON, G.F., Metal Science 10, 307 (1976).

20. AHLQUIST, C.N., GASCA-NERI, R., NIX, W.D., Acta Metall. 18, 663 (1970).

21. BLUM, W., Scripta Metall. 16, 1353 (1982).

TABLE I

ALLOY	HEAT	ANNEALING TREATMENT	GRAIN SIZE
A800	8144	solution *	80 um
A800	8523	mill **	5 um
316SS	--	solution *	50 um

* 1 h at 1450 K
** 1 h at 1280 K

CAPTIONS TO FIGURES

Figure 1. Schematic of strain transients observed in A800 and 316SS.
Figure 2. Results from a typical dip test series.
Figure 3. Characteristic creep behavior of A800 and 316SS.
Figure 4. Kinematic variable at steady state in (a) A800 and (b) 316SS.

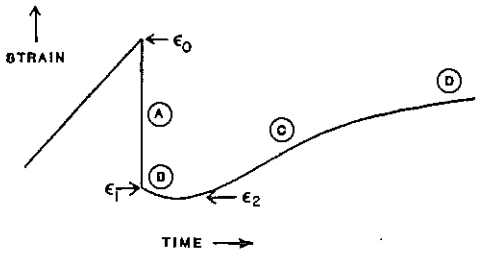

Figure 1.

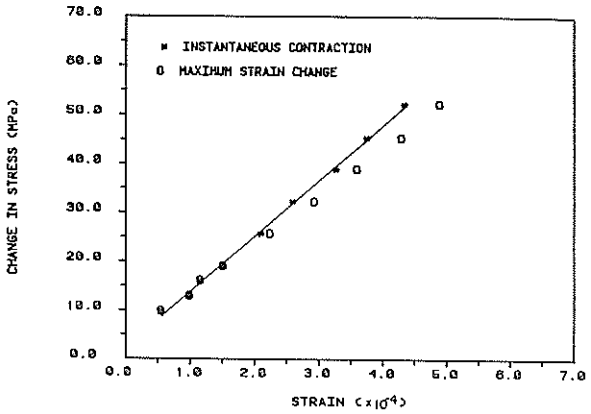

Figure 2.

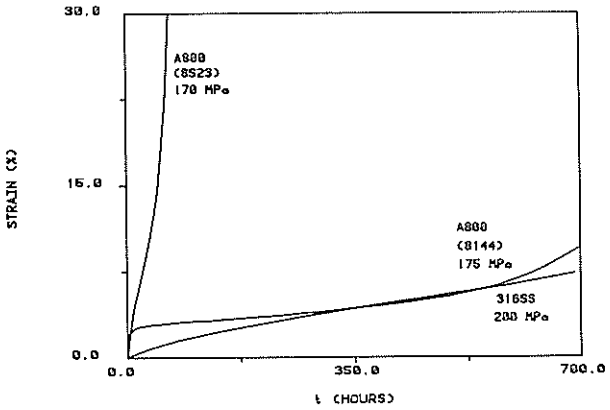

Figure 3.

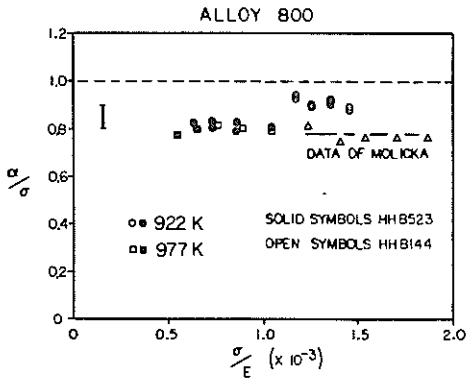

Figure 4a.

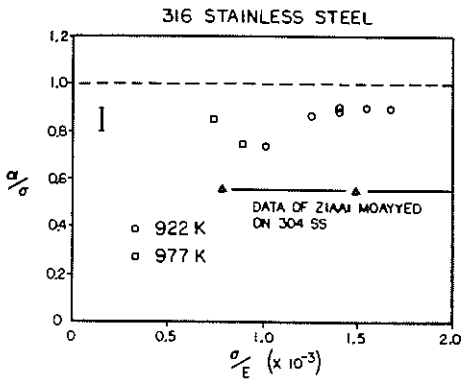

Figure 4b.